Journal of Inorganic Biochemistry 198 (2019) 110718

Contents lists available at ScienceDirect

Journal of Inorganic Biochemistry

journal homepage: www.elsevier.com/locate/jinorgbio

Determination of the magnetic properties and orientation of the heme axial ligands of PpcA from *Geobacter metallireducens* by paramagnetic NMR

Tomás M. Fernandes[a], Leonor Morgado[a], Carlos A. Salgueiro[a,*], David L. Turner[b,*]

[a] UCIBIO-Requimte, Departamento de Química, Faculdade de Ciências e Tecnologia, Universidade NOVA de Lisboa, Campus Caparica, 2829-516 Caparica, Portugal
[b] Instituto de Tecnologia Química e Biológica António Xavier, Universidade NOVA de Lisboa, Avenida da República (EAN), 2780-157 Oeiras, Portugal

ARTICLE INFO

Keywords:
Geobacter
Multiheme cytochrome
NMR
Paramagnetic systems

ABSTRACT

The rising interest in the use of *Geobacter* bacteria for biotechnological applications demands a deep understanding of how these bacteria are able to thrive in a variety of environments and perform extracellular electron transfer. The *Geobacter metallireducens* bacterium can couple the oxidation of a wide range of compounds to the reduction of several extracellular acceptors, including heavy metals, toxic organic compounds or electrode surfaces. The periplasmic *c*-type cytochrome PpcA from this bacterium is a member of a family composed of five periplasmic triheme cytochromes, which are important to bridge the electron transfer between the cytoplasm and the extracellular environment. To better understand the functional mechanism of PpcA it is essential to obtain structural data for this cytochrome. In this work, the geometry of the heme axial ligands, as well as the magnetic properties of the hemes were determined for the oxidized form of the cytochrome, using the ^{13}C NMR chemical shifts of the heme α-substituents. The results were further compared with those previously obtained for the homologous cytochrome from *Geobacter sulfurreducens*. The orientations of the axial histidine planes and the magnetic properties of the hemes are conserved in both proteins. Overall, the results obtained allowed the definition of the orientation of the magnetic axes of PpcA from *G. metallireducens*, which will be used as constraints to assist the solution structure determination of the cytochrome in the oxidized form.

1. Introduction

The bacterium *Geobacter metallireducens* has an impressive respiratory versatility [1]. In fact, in addition to the more frequent respiratory processes that culminate with the intracellular reduction of terminal acceptors, it can also utilize extracellular compounds [2]. Some extracellular terminal acceptors are either toxic or radioactive [3–8] and for that reason several bioremediation applications are being developed for their removal from the environment [9,10]. Moreover, *G. metallireducens* produces one of the highest current densities in microbial fuel cells, making it an interesting target for bioenergy applications [11,12]. To develop these biotechnological applications it is important to understand the structural/functional relationships of the different electron transfer components of the so-called extracellular electron transfer (EET) pathways. The bacterium *G. metallireducens* shares several metabolic features with *Geobacter sulfurreducens* but it is capable of oxidizing a wider range of organic compounds, allowing the bacterium to strive in more differentiated environments [1]. These remarkable features, together with the recent development of a genetic system for the bacterium [13], have refocused attention on this organism within the framework of the mentioned applications.

The genome of *G. metallireducens* encodes for 91 *c*-type cytochromes, with 65 having more than one heme binding site [1]. Several cytochromes from the inner-membrane, periplasm and outer-membrane are conserved compared to *G. sulfurreducens* [1]. More specifically, the periplasmic family of five triheme cytochromes, crucial to bridge the electron flow between the inner- and outer-membrane electron transfer components, is conserved. For this reason, this family of cytochromes can be explored to develop rational *Geobacter*-mutated strains with increased respiratory rates and optimal biotechnological applications.

The periplasmic *c*-type cytochrome PpcA from *G. metallireducens* contains 70 amino acids (molecular weight of 9.7 kDa) and was recently characterized [14,15]. As in the case of its homologue from *G. sulfurreducens*, PpcA from *G. metallireducens* contains three *c*-type low-spin heme groups with bis-histidinyl axial coordination, being diamagnetic (S = 0) and paramagnetic (S = 1/2) in the reduced and oxidized states, respectively. However, the global redox potential of PpcA from *G. metallireducens* is less negative [14,15]. The detailed thermodynamic characterization of the two cytochromes showed that they share similar redox potentials for heme IV, but distinct ones for hemes I and III (the

* Corresponding authors.
E-mail addresses: csalgueiro@fct.unl.pt (C.A. Salgueiro), turner@itqb.unl.pt (D.L. Turner).

https://doi.org/10.1016/j.jinorgbio.2019.110718
Received 27 March 2019; Received in revised form 9 May 2019; Accepted 13 May 2019
Available online 17 May 2019
0162-0134/

numbering of the hemes derives from the superimposition of the hemes in cytochromes c_7 with those of the structurally homologous tetraheme cytochromes c_3 [16]).

These differences are most likely related with predicted structural differences near hemes I and III [15]. In order to further confirm this hypothesis it is necessary to determine the structure of the cytochrome. NMR is a particularly suitable technique for this goal and structure calculation protocols have been established [17,18]. Either in the reduced or oxidized form, in addition to the standard protocols typically used to determine the solution structure of non-hemic proteins, in the case of cytochromes it is also necessary to assign the heme substituents signals and determine the related structural restraints [19]. However, in the paramagnetic oxidized form, the solution structure determination is even more challenging. In fact, in addition to the heme ring-current effects, the paramagnetic contributions caused by the presence of unpaired electrons on the heme irons strongly contribute to the observed chemical shift of the heme substituents and neighbor amino acids. In fact, the same type of signals are (i) differently affected by the paramagnetic center(s), (ii) show different levels of broadness and (iii) are spread over the entire NMR spectral width, making their assignment more complex. Furthermore, in the paramagnetic state, the dipolar couplings caused by the unpaired electrons increase the relaxation rates of nearby protons, reducing Nuclear Overhauser Effect (NOE) intensities [17]. Consequently, it is also necessary to correct this paramagnetic leakage [17,20,21]. In the particular case of the heme axial ligands, the broadness of their side chain signals is enormous, which impairs the observation of NOEs. Particularly, for bis-histidinyl axial coordinated hemes, the orientation of the axial histidine rings cannot be determined from the NOE constraints used for structure calculation. Instead, this information can be indirectly obtained from the pattern of paramagnetic shifts of the heme(s) α-substituents [22,23] (Fig. 1), that will simultaneously allow the definition of (i) the electron structure of the hemes, (ii) the orientation of the magnetic axes generated by the unpaired electron(s), (iii) the shape of the magnetic susceptibility tensor and (iv) the relative orientation of the aromatic planes of the axial histidines [18,22–30].

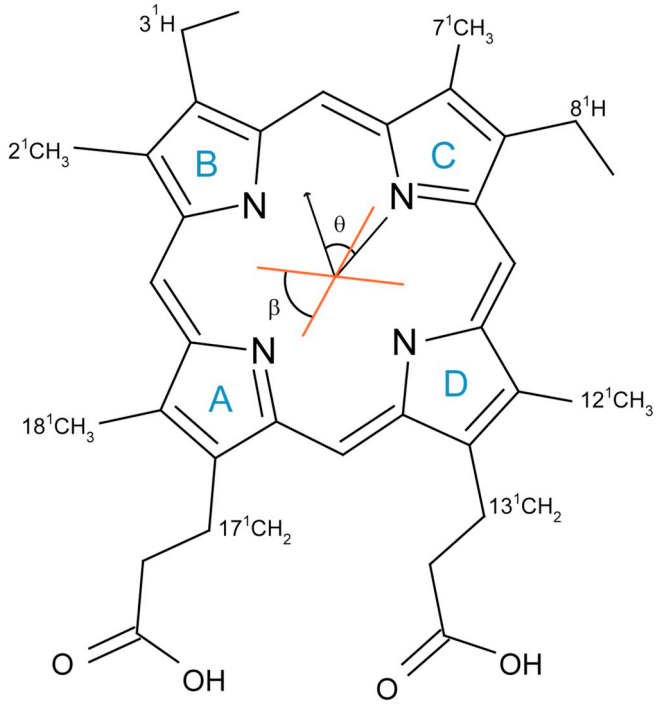

Fig. 1. Diagram of heme *c* showing the parameters β and θ. The heme α-substituents are numbered according to the IUPAC-IUB nomenclature for tetrapyrroles [55]. The heme pyrrole rings are labeled (blue letters) according to the Brookhaven Protein Data Bank standard atom nomenclature for metal-substituted protohemes. The black arrow represents the orientation of the rhombic perturbation and the black line represents the N_C-N_A direction. The two orange lines represent the projection of the axial histidines planes on the heme.

In this work, the paramagnetic chemical shifts of the hemes signals of PpcA from *G. metallireducens* were used to (i) determine the electronic structure of the three hemes, (ii) define the orientation of the aromatic rings planes of the axial histidines and (iii) establish the orientation of the magnetic axes relative to each heme group. The results were compared to the ones previously obtained for the homologous cytochrome from *G. sulfurreducens* [27] and constitute the foundations towards the determination of the solution structure of the oxidized form of PpcA from *G. metallireducens*.

2. Materials and methods

2.1. Expression and purification of triheme cytochrome PpcA from G. metallireducens

Natural abundance and ^{13}C isotopic labeled samples of PpcA from *G. metallireducens* were produced as previously described [15]. Briefly, *Escherichia coli* BL21 (DE3) cells previously transformed with the plasmid pEC86 (encoding for the cytochrome *c* maturation gene cluster *ccmABCDEFGH* and a chloramphenicol resistance gene), were co-transformed with the plasmid pCSGmet2902 (containing the gene *Gmet_2902,* encoding for *G. metallireducens* PpcA and carrying an ampicillin resistance gene). The cells were then grown aerobically to mid-exponential phase at 30 °C in 2xYT media, supplemented with chloramphenicol and ampicillin. On one hand, for production of natural abundance samples, the protein expression was induced with 10 μM of isopropyl β-D-thiogalactoside (IPTG) and cultures growth overnight at 30 °C. On the other hand, to produce ^{13}C isotopic labeled samples, the cells were collected and resuspended in minimal media supplied with 4 g/L $^{13}C_6H_{12}O_6$ (together with 1 mM of the heme precursor δ-aminolevulinic acid, trace amounts of metal salts, biotin and thiamine), as ^{13}C source. In minimal media, the cells were then incubated at 30 °C and protein expression was induced with 100 μM IPTG after 2 h. In both cases, following overnight incubation, cells were harvested by centrifugation at 4000 × *g* for 20 min and the periplasmic fraction was isolated using lysis buffer (100 mM Tris-HCl (pH 8.0), 0.5 mM EDTA, 20% sucrose and 0.5 mg/mL lysozyme). The periplasmic fraction was recovered by centrifugation at 14700 × *g*, at 4 °C for 20 min. The supernatant was further ultracentrifuged at 225000 × *g*, at 4 °C for 1 h. The final supernatant obtained was dialyzed against 2 × 4.5 L of 10 mM Tris-HCl (pH 8.0) and loaded onto 2 × 5 mL Bio-Scale™ Mini UNOsphere™ S cartridges (BioRad), equilibrated with the same buffer. The protein was eluted with a sodium chloride gradient (0–300 mM) and the obtained fraction was concentrated to 1 mL before injection in a Superdex 75 molecular exclusion column (GE Healthcare), equilibrated with 100 mM sodium phosphate buffer (pH 8.0). Protein purity was evaluated by Coomassie stained SDS-PAGE. The concentration of the cytochrome was determined by measuring the absorbance of the reduced form at 552 nm, using the extinction coefficient of 118 mM^{-1} cm^{-1} [15].

2.2. NMR spectroscopy

We have previously shown that the integrity of PpcA from *G. metallireducens* is maintained after lyophilization [14,15]. Therefore, natural abundance samples were lyophilized twice and prepared either at 80 μM (samples for 2D ^{1}H-EXchange SpectroscopY (EXSY) experiments) or 1 mM of protein (samples for 2D ^{1}H,^{13}C-Heteronuclear Single Quantum Coherence (HSQC), 2D ^{1}H-Nuclear Overhauser Effect SpectroscopY (NOESY) and 2D ^{1}H-TOtal Correlation SpectroscopY (TOCSY) experiments), in 80 mM phosphate buffer, pH 8.0, with NaCl (250 mM final ionic strength) in pure ^2H_2O (99.9% atom, CIL isotopes). ^{13}C

labeled samples were prepared with the same buffer and 1 mM of protein, in 92% H_2O/8% ^2H_2O. The partially oxidized samples were prepared using the following protocol: first, the NMR tubes were sealed with a gas-tight serum cap and the air was flushed out to avoid possible oxidation of the samples. The samples were then reduced directly in the NMR tube with gaseous hydrogen in the presence of catalytic amounts of hydrogenase from *Desulfovibrio vulgaris* (Hildenborough). The hydrogen was then removed from the NMR tube with nitrogen and controlled amounts of air were added into the sample with a Hamilton syringe. The pH values of all the samples were verified with a glass micro electrode. All the NMR experiments were acquired on a Bruker Avance III 600 MHz spectrometer equipped with a triple-resonance cryoprobe (TCI) at 288 and 298 K. The ^{1}H chemical shifts were calibrated using the water signal as internal reference and the ^{13}C chemical shifts were calibrated through indirect referencing [31]. All the spectra were processed using TopSpin3.5.7™ (Bruker BioSpin, Karlsruhe, Germany) and analyzed with the program Sparky (T. D. Goddard and D.G. Kneller, SPARKY 3, University of California, San Francisco). For the assignment of the heme α-substituents of the protein in the fully oxidized state, the following set of 2D NMR experiments was acquired for natural abundance samples: 2D ^{1}H,^{13}C-HSQC, 2D ^{1}H-NOESY and 2D ^{1}H-TOCSY. The 2D ^{1}H,^{13}C-HSQC spectra were acquired collecting 4096 (t_2) × 256 (t_1) data points to cover a sweep width of 28.8 kHz in the ^{1}H dimension and 52.8 kHz in the ^{13}C dimension, with 360 scans per increment. The 2D ^{1}H-NOESY spectra were acquired with a mixing time of 80 ms, collecting 4096 (t_2) × 512 (t_1) data points to cover a sweep width of 28.8 kHz, with 200 scans per increment. The 2D ^{1}H-TOCSY spectra were acquired with a mixing time of 45 ms, collecting 2048 (t_2) × 512 (t_1) data points to cover a sweep width of 28.8 kHz, with 160 scans per increment. Moreover, to help discriminate between the polypeptide chain and heme signals, 2D ^{1}H,^{13}C-HSQC spectra were acquired on ^{13}C labeled samples. These spectra were acquired collecting 4096 (t_2) × 256 (t_1) data points to cover a sweep width of 28.8 kHz in the ^{1}H dimension and 52.8 kHz in the ^{13}C dimension, with 8 scans per increment. Finally, 2D ^{1}H-EXSY spectra were acquired at different levels of oxidation with a mixing time of 25 ms, collecting 2048 (t_2) × 256 (t_1) data points to cover a sweep width of 27.5 kHz, with 256 scans per increment. 1D ^{1}H -NMR spectra were obtained before and after each 2D NMR spectrum to check for any changes in the oxidation level of the sample during the 2D NMR experiment. The 1D ^{1}H-NMR spectra were acquired with water pre-saturation collecting 32 k data points to cover a spectral width of 33 kHz. All NMR experiments set-ups are part of the Bruker standard pulse sequence library. The procedure used for the specific assignment of the heme signals is described in Section 3.1.

2.3. Determination of the axial ligands geometry

The ^{13}C chemical shifts of the heme α-substituents of PpcA at 288 and 298 K were fitted to a model of the heme molecular orbitals, which are semi-empirically related to the axial ligand geometry. The model used in this work to obtain structural information on the heme axial ligands was previously described [30]. Briefly, when the heme is oxidized the unpaired electron on the iron *d*-orbitals is partially delocalized into the porphyrin π-orbitals. The ^{13}C nuclei of the α-substituents of the hemes experience Fermi contact shifts proportional to the fraction of occupancy of the unpaired electron in the adjacent carbon belonging to the conjugated π system. The shape of the frontier molecular orbitals of the porphyrin can therefore be deduced from the pattern of paramagnetic shifts. This shape is defined by the orientation of the rhombic perturbation (θ, also labeled as π in the literature [32]) that mixes the frontier molecular orbitals of the heme and the energy splitting of these orbitals (ΔE). The orientation of the rhombic perturbation is known to agree with the orientation of the bisector of the acute angle (β) defined by the normal to the planes of the axial ligands in several bis-histidinyl cytochromes [33]. This orientation is defined relative to the N_C-N_A axis of the porphyrin, with positive angles between N_C-N_B-N_A (Fig. 1) [29]. The energy splitting parameter ΔE has a similar value to the rhombic splitting of the Kramers doublets that arise from mixing d_{xz} and d_{yz} orbitals of the iron when it is in a cubic crystal field with axial and rhombic distortions, and was found to relate to the acute angle β between the axial ligand planes via the empirical equation $\Delta E = (5 + \cos 4\theta)\cos\beta$ [22]. This information allows the magnetic axes to be placed relative to the heme frame, considering that the χ_{zz} axis is normal to the heme plane and that the rhombic perturbation and the χ_{yy} axis are related by a counter-rotation [23,26,28]. Several studies of cytochromes with hemes with various distortions and χ_{zz} axes tilted away from the normal to the heme plane have demonstrated a good correlation between the axial ligand orientations, the magnetic susceptibility tensor, and the heme molecular orbitals, thus confirming the validity of the approach [22,23,29]. The fits were performed in Microsoft Excel and the errors of the parameters were assessed by random variation of the input chemical shifts with a standard deviation of 1 ppm. Average values of chemical shifts measured in several cytochromes were used as diamagnetic reference (12.1 ppm for methyls, 36.5 ppm for thioethers and 22.5 ppm for α-propionates [29]) and the hyperfine coupling constant was fixed at −36 MHz [22]. The results were cross-checked by an empirical fit of the ^{1}H chemical shifts of the heme methyl groups at 298 K [33].

3. Results and discussion

3.1. Resonance assignment of the heme α-substituents

The assignment of the heme α-substituents in the oxidized state benefits from the unambiguous assignment of the heme methyls in the fully reduced state of the protein [15]. These signals can be followed to their final position in the fully oxidized state using 2D ^{1}H-EXSY NMR spectra, a procedure well established for low-spin multiheme cytochromes, as previously demonstrated [34,35]. In the particular case of PpcA from *G. metallireducens*, only nine heme methyl signals could be assigned to their final position in the paramagnetic form of the protein: 2^1CH_3, 12^1CH_3 and 18^1CH_3 from heme I, 7^1CH_3 and 12^1CH_3 from heme III and all the four heme methyls from heme IV. The remaining three heme methyl signals ($7^1H_3^I$, $2^1CH_3^{III}$ and $18^1CH_3^{III}$) have small paramagnetic contributions and appear in crowded regions of the spectra (Fig. 2), making it difficult to assign via 2D ^{1}H-EXSY NMR experiments. Thus, these heme methyls, together with the remaining α-substituents (the thioether methines 3^1H and 8^1H, as well as the α-propionates 13^1CH_2 and 17^1CH_2 for all three hemes), were specifically assigned in the oxidized state by combining data from 2D ^{1}H,^{13}C-HSQC, 2D ^{1}H-NOESY and 2D ^{1}H-TOCSY experiments, using strategies that were previously described [30,36–38]. Briefly, the combined analysis of 2D ^{1}H,^{13}C-HSQC spectra acquired for labeled and unlabeled samples allows for a straight discrimination between the heme substituents and polypeptide chain signals. Since the heme precursor (δ-aminolevulinic acid) added into the minimal media is not labeled, the heme signals are not observable in spectra acquired with a relatively small number of accumulations in ^{13}C labeled samples. Therefore, by simple comparison of the two NMR spectra, the heme substituents signals and those of the polypetide chain can be discriminated. After this procedure, the assignments are obtained using the intraheme TOCSY and NOESY connectivities, as previously described [30,36,38]. Fig. 2 and Table 1 report the assignment of 93% of the paramagnetic α-substituents. The small fraction of unassigned signals is located in highly crowded spectral regions and could not be assigned with confidence, even using the different strategies presented.

3.2. Geometry and magnetic properties of the axial ligands of PpcA

The model presented to analyze the ^{13}C chemical shifts of the heme signals in terms of the heme molecular orbitals is only valid for low-spin

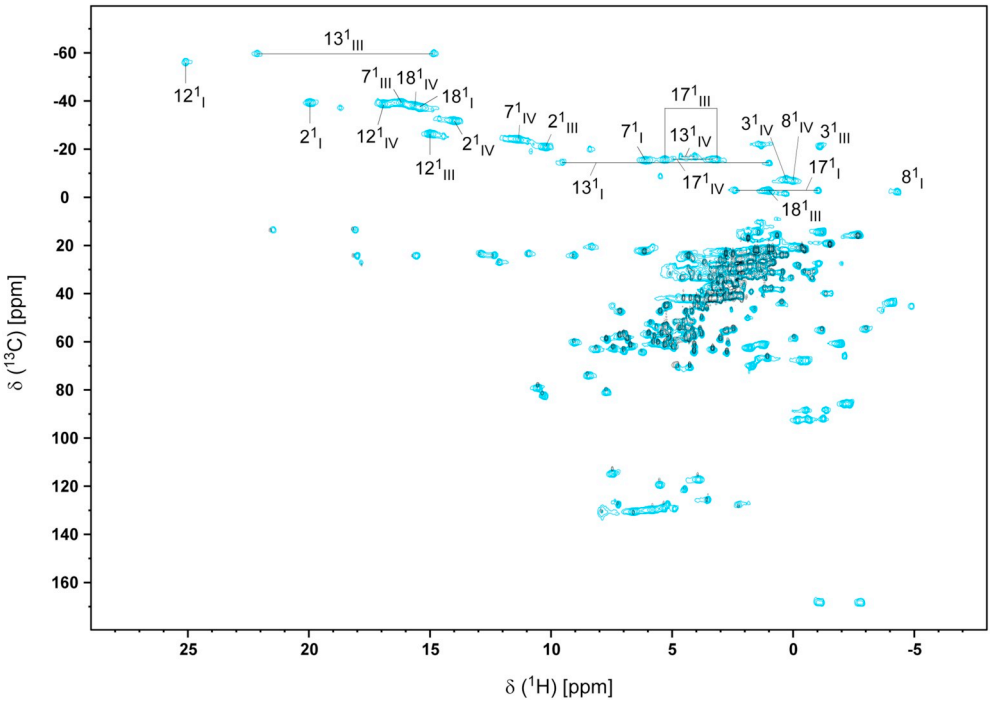

Fig. 2. Superimposed 2D $^{1}H,^{13}C$-HSQC spectra of labeled (black contours) and unlabeled (blue contours) samples of PpcA from *G. metallireducens* in the oxidized state at pH 8.1 and 298 K. The heme substituents are labeled according to the IUPAC-IUB nomenclature [55]. Roman numerals indicate the hemes in their order of attachment to the CXXCH motif in the polypeptide chain. The peaks of the protons connected to the same carbon atoms (CH_2 groups) are linked by a straight line. The detailed assignment is presented in Table 1.

Table 1
^{1}H and ^{13}C chemical shifts (ppm) of the α-substituents of the three hemes of PpcA from *G. metallireducens* at 288 and 298 K (pH 8.1, 250 mM ionic strength).

T (K)	Group	Heme I		Heme III		Heme IV	
		^{13}C	^{1}H	^{13}C	^{1}H	^{13}C	^{1}H
288	2^1	−41.77	20.69	−21.81	10.28	−33.11	14.14
	3^1	–	–	−22.90	−1.43	−8.86	0.02
	7^1	−15.60	5.57	−40.97	16.43	−25.29	11.50
	8^1	−3.26	−4.81	–	–	−8.17	−0.29
	12^1	−59.09	25.98	−27.40	15.20	−40.26	17.12
	13^1	−15.89	0.77	−62.60	14.97	−18.47	3.90
			9.79		22.69		4.46
	17^1	−3.07	−1.59	−17.02	3.06	−17.21	3.06
			1.91		5.29		4.82
	18^1	−37.98	15.20	−2.74	0.64	−39.48	15.77
298	2^1	−39.52	19.96	−21.03	10.22	−31.95	13.99
	3^1	–	–	−21.19	−1.13	−7.48	0.29
	7^1	−15.53	6.09	−39.50	16.17	−24.24	11.34
	8^1	−2.34	−4.31	–	–	−6.82	0.00
	12^1	−56.44	25.08	−26.55	14.99	−38.96	16.91
	13^1	−14.55	0.98	−60.06	14.84	−17.14	4.05
			9.52		22.14		4.64
	17^1	−3.03	−1.05	−15.89	3.15	−16.08	3.31
			2.39		5.29		4.98
	18^1	−37.48	15.42	−2.93	1.01	−38.22	15.62

hemes [30]. The cytochrome PpcA was previously reported to be low-spin in the reduced (S = 0) and oxidized (S = 1/2) states [15]. This was independently confirmed in this work by measuring the temperature dependence of the heme methyl substituents (Supplementary Fig. S1). The data obtained showed that all heme methyl signals display a linear dependence of their chemical shifts with temperature, indicating that there are no significant contributions from high-spin states [39].

The orientations of the hemes axial histidines planes were deduced from the pattern of ^{13}C NMR paramagnetic shifts of the hemes α-substituents at two different temperatures (288 and 298 K). The results reported in Fig. 3 and Table 2 show that the geometries of the axial histidines planes are different for the three heme groups of PpcA from *G. metallireducens*. This is observed for the projection on the heme plane of the acute angle between the heme axial histidine planes (β), as well as for the orientation of those planes relative to the N_C-N_A axis of the porphyrin. Furthermore, the orientation of the rhombic perturbation (θ) is also represented and the length of the line is proportional to the magnitude of the orbital energy splitting between the frontier molecular orbitals (ΔE). Lower ΔE values result in more axial hemes, whereas higher ΔE values result in more rhombic ones. These results were confirmed by applying the empirical equation δ_i (ppm) = cosβ [38 $\sin^2(\theta_i - \Phi) - 4.1\cos^2(\theta_i - \Phi) - 15.9] + 13.8$ [33] to the ^{1}H chemical shifts of the heme methyl groups at 298 K, where β is the acute angle between the heme axial histidine planes, θ_i refers to the position of the *i*th methyl substituent (average of the methyl protons positions [33]) and Φ is equivalent to the angle between the bisector of the angle β and the N_C-N_A axis of the porphyrin. Fig. 3 also shows that the orientations of the axial histidines planes are highly similar between the homologous cytochromes from *G. metallireducens* and *G. sulfurreducens*. This is expected considering the high sequence identity (80%) shared between the two proteins. In both cytochromes, (i) heme I presents a similar orientation between the axial histidine planes (similar β values), (ii) heme III is the most rhombic of the three hemes (higher ΔE values) and shows a narrow distribution in the acute angle between the histidine planes (β) and a θ angle close to 70° and (iii) in heme IV, the higher β values (> 80°) indicate that the histidine planes are almost perpendicular to each other. The magnetic properties of the hemes are also conserved.

Despite this, the redox potentials of the two homologous cytochromes showed considerable differences, with those of PpcA from *G. metallireducens* being considerably less negative [14]. There are several factors capable of tuning the hemes reduction potentials, namely (i) the number and nature of protein axial ligands to iron [40–42], (ii) the heme solvent exposure [43–45], (iii) the distribution of polar and charged groups in the heme neighborhood [46,47], (iv) the axial imidazole ligand plane orientation (particularly in the case of bis-histidinyl coordinated hemes) [48,49], among others (for a review, see [50]). The axial imidazole ligand plane orientation affects the heme reduction potential by altering the orientation and stability of the heme iron *d*-orbitals [48,49]. The high degree of conservation of the axial histidines planes of the homologous PpcA cytochromes indicates that the differences in the redox potentials are not related with alterations in the orientation of the hemes axial ligands (Table 2 and Fig. 3) and are

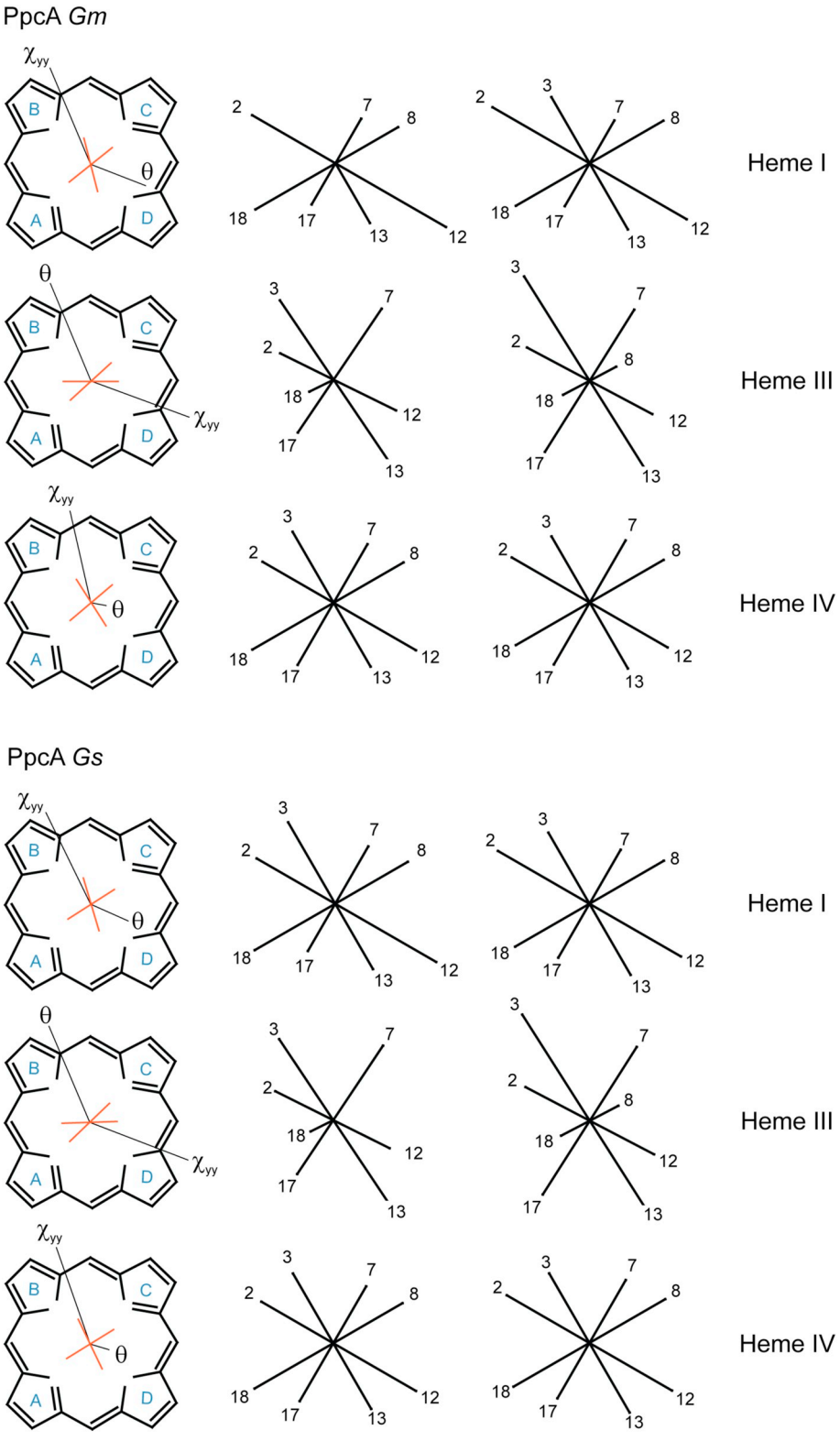

Fig. 3. Orientation of the heme axial ligands, and experimental and calculated shifts of the hemes α-substituents of PpcA from *G. metallireducens* (*Gm*). The orientations of the axial histidines planes determined in this work are represented in the first column (in orange), together with the orientation of the rhombic perturbation (θ) and the χ_{yy} magnetic axis for each heme. The length of the line corresponding to the rhombic perturbation is proportional to the magnitude of the orbital energy splitting between the frontier molecular orbitals (ΔE). The last two columns represent the experimental and calculated ^{13}C NMR paramagnetic shifts of the heme α-substituents at 298 K, respectively (also see Supplementary Table S1). Each line is oriented from the center of the heme to the respective carbon with length proportional to the paramagnetic shift. The heme pyrrole rings are identified (blue letters) according to the Brookhaven Protein Data Bank standard atom nomenclature for metal-substituted protohemes and the heme α-substituents are identified according to the IUPAC-IUB nomenclature [55]. The axes are defined relative to the N_C-N_A vector, with a positive angle for a rotation in counter clockwise direction. The same set of data is also presented for PpcA from *G. sulfurreducens* (*Gs*) [27], for comparison.

probably explained by the non-conserved residues located in the vicinity of hemes I and III [15].

The orientation of the heme coordinating histidines determined in the present work for the fully oxidized cytochrome might differ from those in the fully reduced protein. The structural data obtained for triheme cytochromes in both redox states showed that the most significant structural changes are mainly confined to the side chains of the non-axial heme coordinating residues. However, redox-linked conformation changes associated to the orientation of the heme axial histidines have also been detected. This is the case of the triheme cytochrome c_7 from *Desulfuromonas acetoxidans* [16,51,52] and PpcA from *G. sulfurreducens* [53]. Thus, given the high sequence identity between the homologous cytochromes from *G. metallireducens* and *G. sulfurreducens*, it is expected that similar redox-linked conformational changes in the axial ligands of PpcA from *G. metallireducens* will be found. The determination of the structure of the reduced form of PpcA from *G.*

Table 2
Molecular orbital parameters obtained by fitting of the ^{13}C signals of the heme α-substituents of PpcA from *G. metallireducens* (*Gm*). The standard errors associated with the molecular orbital parameters were calculated assuming that the chemical shifts have an experimental uncertainty of ± 1 ppm [33]. The parameter β was calculated from the energy splitting of the molecular orbitals using an empirical equation (see Section 2.3). The molecular orbital parameters of PpcA from *G. sulfurreducens* (*Gs*) [27] are also presented, for comparison.

Protein	Parameters	Heme I	Heme III	Heme IV
PpcA Gm	θ (°)	−66.9 ± 0.4	66.1 ± 0.2	−56.8 ± 1.2
	ΔE (J mol^{-1})	2034 ± 25	3615 ± 48	582 ± 21
	β (°)	65.8 ± 0.8	42.5 ± 1.5	82.3 ± 0.6
PpcA *Gs* [27]	θ (°)	−70.0	66.9	−63.3
	ΔE (J mol^{-1})	1350	3540	670
	β (°)	73.7	41.5	83.5

metallireducens is therefore required to confirm this redox-linked dependency of the axial ligands.

4. Conclusions

In this work, the assignment of the hemes α-substituents of PpcA from *G. metallireducens* in the oxidized state, together with the use of a model of the heme molecular orbitals, allowed the determination of the hemes axial histidine planes and magnetic properties. The results showed that the hemes axial histidine planes and the magnetic properties are conserved when compared with the homologous cytochrome from *G. sulfurreducens*. As noted above, a previous study demonstrated that there are significant structural differences between the homologous PpcA cytochromes, located in the vicinities of hemes I and III [15]. Another study demonstrated that the reduction potential of heme IV is almost identical in both proteins, whereas the heme I and III reduction potentials differ considerably [14]. Therefore, it is believed that the overall differences in reduction potential between the two homologous cytochromes are most likely related with structural differences located near hemes I and III. The results obtained demonstrated that the orientation of the axial ligands is not the factor that determines the differences in the reduction potential of the two proteins.

The determination of the solution structure of the cytochrome from *G. metallireducens* in both redox states will be useful not only to map redox-linked conformation changes, but also to elucidate the origin of the differences observed in the redox properties of the two cytochromes.

Accurate information on the geometry of the heme axial ligands is essential for the solution determination of structures of paramagnetic heme proteins [18,54]. This is particularly relevant for the heme ligands since paramagnetic relaxation bleaches NOE connectivities to the imidazole protons of the axial histidines, leaving the geometry of the heme pocket poorly defined. The determination of the magnetic properties of PpcA from *G. metallireducens* presented in this work will allow future estimations of pseudocontact shifts, a crucial step to calculate paramagnetic structural constraints that will be included in the refinement process of the solution structure for the oxidized form of the cytochrome.

Declaration of Competing Interest

There are no conflicts to declare.

Acknowledgments

This work was supported by Fundação para a Ciência e Tecnologia (FCT) through the following grants: SFRH/BPD/114848/2016 (to LM), PTDC/BBB-BQB/3554/2014, PTDC/BBB-BQB/4178/2014 and PTDC/BIA-BQM/31981/2017 (to CAS). This work was also supported by the Applied Molecular Biosciences Unit-UCIBIO which is financed by national funds from FCT/MEC (UID/Multi/04378/2019). The NMR spectrometers are part of Rede Nacional de RMN (PTNMR), supported by FCT-MCTES (ROTEIRO/0031/2013 - PINFRA/22161/2016) co-funded by FEDER through COMPETE 2020, POCI, and PORL and FCT through PIDDAC.

Author contribution

TMF and LM prepared the samples and acquired the NMR experiments. All the authors participated in the data analysis and treatment. TMF prepared all the figures. CAS and TMF wrote the manuscript. DLT critically read and revised the manuscript.

Appendix A. Supplementary data

Supplementary data to this article can be found online at https://doi.org/10.1016/j.jinorgbio.2019.110718.

References

[1] M. Aklujkar, J. Krushkal, G. DiBartolo, A. Lapidus, M.L. Land, D.R. Lovley, The genome sequence of *Geobacter metallireducens*: features of metabolism, physiology and regulation common and dissimilar to *Geobacter sulfurreducens*, BMC Microbiol. 9 (2009) 109.
[2] D.R. Lovley, Dissimilatory metal reduction, Annu. Rev. Microbiol. 47 (1993) 263–290.
[3] J.D. Coates, J. Woodward, J. Allen, P. Philp, D.R. Lovley, Anaerobic degradation of polycyclic aromatic hydrocarbons and alkanes in petroleum-contaminated marine harbor sediments, Appl. Environ. Microbiol. 63 (1997) 3589–3593.
[4] K.B. Gregory, D.R. Lovley, Remediation and recovery of uranium from contaminated subsurface environments with electrodes, Environ. Sci. Technol. 39 (2005) 8943–8947.
[5] D.R. Lovley, M.J. Baedecker, D.J. Lonergan, I.M. Cozzarelli, E.J.P. Phillips, D.I. Siegel, Oxidation of aromatic contaminants coupled to microbial iron reduction, Nature 339 (1989) 297–300.
[6] A.L. N'Guessan, H.A. Vrionis, C.T. Resch, P.E. Long, D.R. Lovley, Sustained removal of uranium from contaminated groundwater following stimulation of dissimilatory metal reduction, Environ. Sci. Technol. 42 (2008) 2999–3004.
[7] K.H. Williams, P.E. Long, J.A. Davis, M.J. Wilkins, A.L. N'Guessan, C.I. Steefel, L. Yang, D. Newcomer, F.A. Spane, L.J. Kerkhof, L. McGuinness, R. Dayvault, D.R. Lovley, Acetate availability and its influence on sustainable bioremediation of uranium-contaminated groundwater, Geomicrobiol J. 28 (2011) 519–539.
[8] T. Zhang, S.M. Gannon, K.P. Nevin, A.E. Franks, D.R. Lovley, Stimulating the anaerobic degradation of aromatic hydrocarbons in contaminated sediments by providing an electrode as the electron acceptor, Environ. Microbiol. 12 (2010) 1011–1020.
[9] R.T. Anderson, H.A. Vrionis, I. Ortiz-Bernad, C.T. Resch, P.E. Long, R. Dayvault, K. Karp, S. Marutzky, D.R. Metzler, A. Peacock, D.C. White, M. Lowe, D.R. Lovley, Stimulating the *in situ* activity of *Geobacter* species to remove uranium from the groundwater of a uranium-contaminated aquifer, Appl. Environ. Microbiol. 69 (2003) 5884–5891.
[10] D.R. Lovley, Cleaning up with genomics: applying molecular biology to bioremediation, Nat. Rev. Microbiol. 1 (2003) 35–44.
[11] D.R. Lovley, Microbial fuel cells: novel microbial physiologies and engineering approaches, Curr. Opin. Biotechnol. 17 (2006) 327–332.
[12] D.R. Lovley, T. Ueki, T. Zhang, N.S. Malvankar, P.M. Shrestha, K.A. Flanagan, M. Aklujkar, J.E. Butler, L. Giloteaux, A.E. Rotaru, D.E. Holmes, A.E. Franks, R. Orellana, C. Risso, K.P. Nevin, *Geobacter*: the microbe electric's physiology, ecology, and practical applications, Adv. Microb. Physiol. 59 (2011) 1–100.
[13] P.L. Tremblay, M. Aklujkar, C. Leang, K.P. Nevin, D. Lovley, A genetic system for *Geobacter metallireducens*: role of the flagellin and pilin in the reduction of Fe(III) oxide, Environ. Microbiol. Rep. 4 (2012) 82–88.
[14] T.M. Fernandes, L. Morgado, C.A. Salgueiro, Thermodynamic and functional characterization of the periplasmic triheme cytochrome PpcA from *Geobacter metallireducens*, Biochem. J. 475 (2018) 2861–2875.
[15] P.C. Portela, T.M. Fernandes, J.M. Dantas, M.R. Ferreira, C.A. Salgueiro, Biochemical and functional insights on the triheme cytochrome PpcA from *Geobacter metallireducens*, Arch. Biochem. Biophys. 644 (2018) 8–16.
[16] D.L. Turner, H.S. Costa, I.B. Coutinho, J. Legall, A.V. Xavier, Assignment of the ligand geometry and redox potentials of the trihaem ferricytochrome c_3 from *Desulfuromonas acetoxidans*, Eur. J. Biochem. 243 (1997) 474–481.
[17] L. Brennan, D.L. Turner, A.C. Messias, M.L. Teodoro, J. LeGall, H. Santos, A.V. Xavier, Structural basis for the network of functional cooperativities in cytochrome c_3 from *Desulfovibrio gigas*: solution structures of the oxidised and reduced states, J. Mol. Biol. 298 (2000) 61–82.
[18] D.L. Turner, L. Brennan, S.G. Chamberlin, R.O. Louro, A.V. Xavier, Determination of solution structures of paramagnetic proteins by NMR, Eur. Biophys. J. 27 (1998)

367–375.
[19] A.C. Messias, D.H. Kastrau, H.S. Costa, J. LeGall, D.L. Turner, H. Santos, A.V. Xavier, Solution structure of *Desulfovibrio vulgaris* (Hildenborough) ferrocytochrome c_3: structural basis for functional cooperativity, J. Mol. Biol. 281 (1998) 719–739.
[20] I. Bertini, A. Donaire, I.C. Felli, A. Rosato, C. Luchinat, From NOESY cross peaks to structural constraints in a paramagnetic metalloprotein, Magn. Reson. Chem. 34 (1996) 948–950.
[21] I. Bertini, C. Luchinat, G. Parigi, R. Pierattelli, NMR spectroscopy of paramagnetic metalloproteins, Chembiochem 6 (2005) 1536–1549.
[22] R.O. Louro, I.J. Correia, L. Brennan, I.B. Coutinho, A.V. Xavier, D.L. Turner, Electronic structure of low-spin ferric porphyrins: ^{13}C NMR studies of the influence of axial ligand orientation, J. Am. Chem. Soc. 120 (1998) 13240–13247.
[23] D.L. Turner, L. Brennan, A.C. Messias, M.L. Teodoro, A.V. Xavier, Correlation of empirical magnetic susceptibility tensors and structure in low-spin haem proteins, Eur. Biophys. J. 29 (2000) 104–112.
[24] L. Banci, I. Bertini, K.L. Bren, M.A. Cremonini, H.B. Gray, C. Luchinat, P. Turano, The use of pseudocontact shifts to refine solution structures of paramagnetic metalloproteins: Met80Ala cyano-cytochrome *c* as an example, J. Biol. Inorg. Chem. 1 (1996) 117–126.
[25] L. Banci, I. Bertini, G. Cavallaro, C. Luchinat, Chemical shift-based constraints for solution structure determination of paramagnetic low-spin heme proteins with bis-His and His-CN axial ligands: the cases of oxidized cytochrome b_5 and Met80Ala cyano-cytochrome *c*, J. Biol. Inorg. Chem. 7 (2002) 416–426.
[26] L. Banci, R. Pierattelli, D.L. Turner, Determination of haem electronic structure in cytochrome b_5 and metcyanomyoglobin, Eur. J. Biochem. 232 (1995) 522–527.
[27] L. Morgado, I.H. Saraiva, R.O. Louro, C.A. Salgueiro, Orientation of the axial ligands and magnetic properties of the hemes in the triheme ferricytochrome PpcA from *G. sulfurreducens* determined by paramagnetic NMR, FEBS Lett. 584 (2010) 3442–3445.
[28] N.V. Shokhirev, F.A. Walker, Co- and counterrotation of magnetic axes and axial ligands in low-spin ferriheme systems, J. Am. Chem. Soc. 120 (1998) 981–990.
[29] D.L. Turner, Determination of haem electronic structure in His-Met cytochromes *c* by ^{13}C-NMR: the effect of the axial ligands, Eur. J. Biochem. 227 (1995) 829–837.
[30] D.L. Turner, C.A. Salgueiro, P. Schenkels, J. Le Gall, A.V. Xavier, Carbon-13 NMR studies of the influence of axial ligand orientation on haem electronic structure, Biochim. Biophys. Acta 1246 (1995) 24–28.
[31] D.S. Wishart, C.G. Bigam, J. Yao, F. Abildgaard, H.J. Dyson, E. Oldfield, J.L. Markley, B.D. Sykes, ^{1}H, ^{13}C and ^{15}N chemical shift referencing in biomolecular NMR, J. Biomol. NMR 6 (1995) 135–140.
[32] I. Bertini, C. Luchinat, G. Parigi, F.A. Walker, Heme methyl ^{1}H chemical shifts as structural parameters in some low-spin ferriheme proteins, J. Biol. Inorg. Chem. 4 (1999) 515–519.
[33] D.L. Turner, Obtaining ligand geometries from paramagnetic shifts in low-spin haem proteins, J. Biol. Inorg. Chem. 5 (2000) 328–332.
[34] J.S. Park, T. Ohmura, K. Kano, T. Sagara, K. Niki, Y. Kyogoku, H. Akutsu, Regulation of the redox order of four hemes by pH in cytochrome c_3 from *D. vulgaris* Miyazaki F, Biochim. Biophys. Acta 1293 (1996) 45–54.
[35] C.A. Salgueiro, D.L. Turner, H. Santos, J. Le Gall, A.V. Xavier, Assignment of the redox potentials to the four haems in *Desulfovibrio vulgaris* cytochrome c_3 by 2D-NMR, FEBS Lett. 314 (1992) 155–158.
[36] J.M. Dantas, I.H. Saraiva, L. Morgado, M.A. Silva, M. Schiffer, C.A. Salgueiro, R.O. Louro, Orientation of the axial ligands and magnetic properties of the hemes in the cytochrome c_7 family from *Geobacter sulfurreducens* determined by paramagnetic NMR, Dalton Trans. 40 (2011) 12713–12718.
[37] L. Morgado, A.P. Fernandes, Y.Y. Londer, M. Bruix, C.A. Salgueiro, One simple step in the identification of the cofactors signals, one giant leap for the solution structure determination of multiheme proteins, Biochem. Biophys. Res. Commun. 393 (2010) 466–470.
[38] C.A. Salgueiro, D.L. Turner, A.V. Xavier, Use of paramagnetic NMR probes for structural analysis in cytochrome c_3 from *Desulfovibrio vulgaris*, Eur. J. Biochem. 244 (1997) 721–734.
[39] D.L. Turner, Evaluation of ^{13}C and ^{1}H Fermi contact shifts in horse cytochrome *c*: the origin of the anti-Curie effect, Eur. J. Biochem. 211 (1993) 563–568.
[40] G. Battistuzzi, M. Borsari, J.A. Cowan, A. Ranieri, M. Sola, Control of cytochrome *c* redox potential: axial ligation and protein environment effects, J. Am. Chem. Soc. 124 (2002) 5315–5324.
[41] G. Liu, W. Shao, S. Zhu, W. Tang, Effects of axial ligand replacement on the redox potential of cytochrome *c*, J. Inorg. Biochem. 60 (1995) 123–131.
[42] P. Rydberg, E. Sigfridsson, U. Ryde, On the role of the axial ligand in heme proteins: a theoretical study, J. Biol. Inorg. Chem. 9 (2004) 203–223.
[43] R.J. Kassner, Theoretical model for the effects of local nonpolar heme environments on the redox potentials in cytochromes, J. Am. Chem. Soc. 95 (1973) 2674–2677.
[44] E. Stellwagen, Haem exposure as the determinate of oxidation-reduction potential of haem proteins, Nature 275 (1978) 73–74.
[45] F.A. Tezcan, J.R. Winkler, H.B. Gray, Effects of ligation and folding on reduction potentials of heme proteins, J. Am. Chem. Soc. 120 (1998) 13383–13388.
[46] J. Mao, K. Hauser, M.R. Gunner, How cytochromes with different folds control heme redox potentials, Biochemistry 42 (2003) 9829–9840.
[47] P. Voigt, E.-W. Knapp, Tuning heme redox potentials in the cytochrome *c* subunit of photosynthetic reaction centers, J. Biol. Chem. 278 (2003) 51993–52001.
[48] S. Sarma, B. Dangi, C. Yan, R.J. DiGate, D.L. Banville, R.D. Guiles, Characterization of a site-directed mutant of cytochrome b_5 designed to alter axial imidazole ligand plane orientation, Biochemistry 36 (1997) 5645–5657.
[49] S. Sarma, R.J. DiGate, D.B. Goodin, C.J. Miller, R.D. Guiles, Effect of axial ligand plane reorientation on electronic and electrochemical properties observed in the A67V mutant of rat cytochrome b_5, Biochemistry 36 (1997) 5658–5668.
[50] P. Hosseinzadeh, Y. Lu, Design and fine-tuning redox potentials of metalloproteins involved in electron transfer in bioenergetics, Biochim. Biophys. Acta 1857 (2016) 557–581.
[51] M. Assfalg, L. Banci, I. Bertini, M. Bruschi, M.T. Giudici-Orticoni, P. Turano, A proton-NMR investigation of the fully reduced cytochrome c_7 from *Desulfuromonas acetoxidans*, Eur. J. Biochem. 266 (1999) 634–643.
[52] M. Czjzek, P. Arnoux, R. Haser, W. Shepard, Structure of cytochrome c_7 from *Desulfuromonas acetoxidans* at 1.9 Å resolution, Acta Crystallogr. D Biol. Crystallogr. 57 (2001) 670–678.
[53] L. Morgado, M. Bruix, P.R. Pokkuluri, C.A. Salgueiro, D.L. Turner, Redox- and pH-linked conformational changes in triheme cytochrome PpcA from *Geobacter sulfurreducens*, Biochem. J. 474 (2017) 231–246.
[54] L. Banci, I. Bertini, G. Cavallaro, A. Giachetti, C. Luchinat, G. Parigi, Paramagnetism-based restraints for Xplor-NIH, J. Biomol. NMR 28 (2004) 249–261.
[55] G.P. Moss, Nomenclature of tetrapyrroles. Recommendations 1986 IUPAC-IUB joint commission on biochemical nomenclature (JCBN), Eur. J. Biochem. 178 (1988) 277–328.